Electronic Supplementary Material (ESI) for Lab on a Chip.

Supplemental Information:

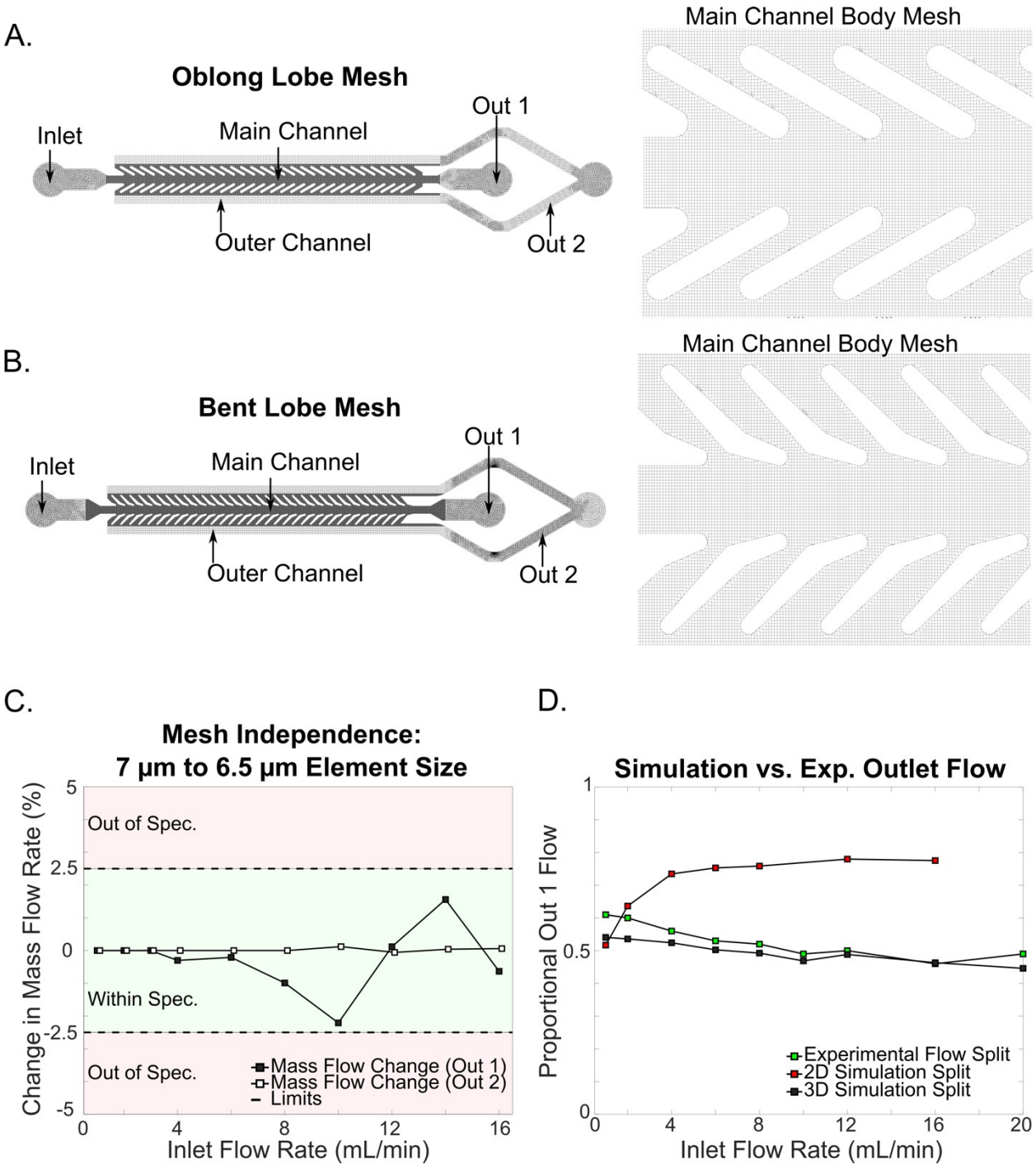

Supplemental Figure 1. Mesh designs obtained from Ansys Meshing for both the **A.** Oblong lobe and **B.** Bent lobe designs. The left side shows the entire mesh designs with labels of the five bodies (Inlet, Outer Channel, Main Channel, Out 1, and Out 2 Bodies). The images on the right show a more detailed perspective of the cartesian meshing pattern for both designs. **C.** Results from a mesh independence study monitoring Out 1 mass flow rate. At all inlet flow rates, the percent change in mass flow rate between meshes using 7 µm and 6.5 µm element sizes stays between +/- 2.5%. **D.** Proportion of mass flow rate exiting through Out 1 vs Inlet mass flow rate for 2D simulations, 3D simulations, and experimental

observation in the Bent lobe device over various inlet flow rates. Unlike 3D simulations, proportional Out 1 flow rate increases as inlet flow rate increases, which does not match experimental observation.

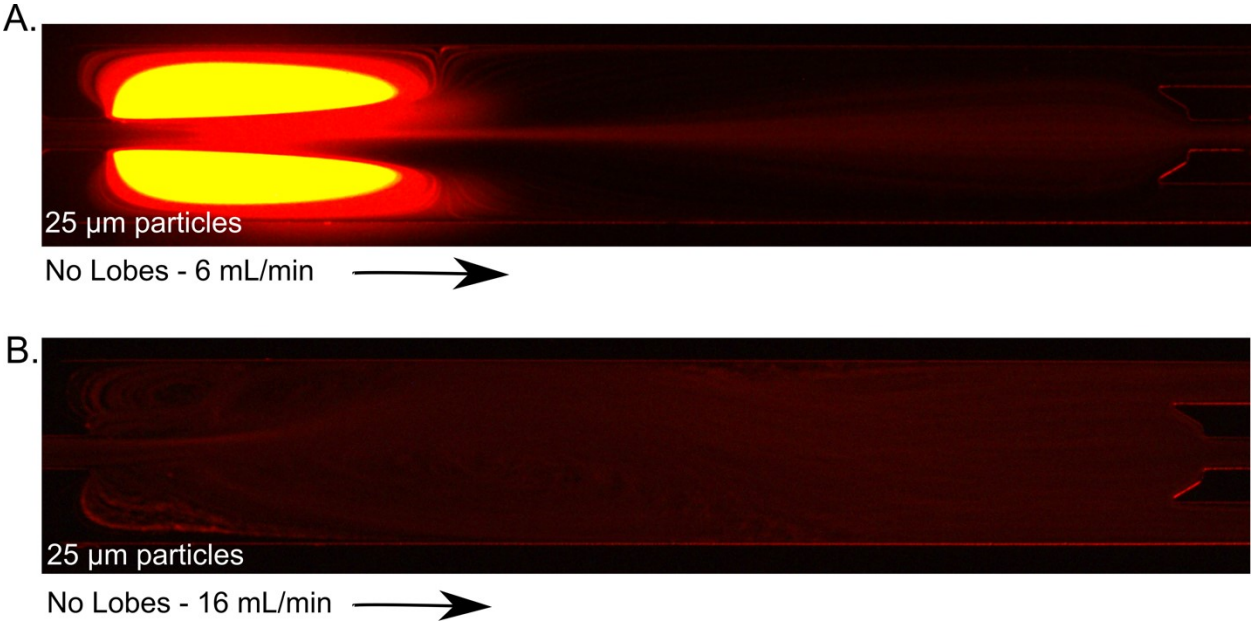

Supplemental Figure 2. Lobe filter design with no lobes running at A. 6 mL/min and B. 16 mL/min inlet flow rates. In both cases, 25 µm particles exit through both outlets.

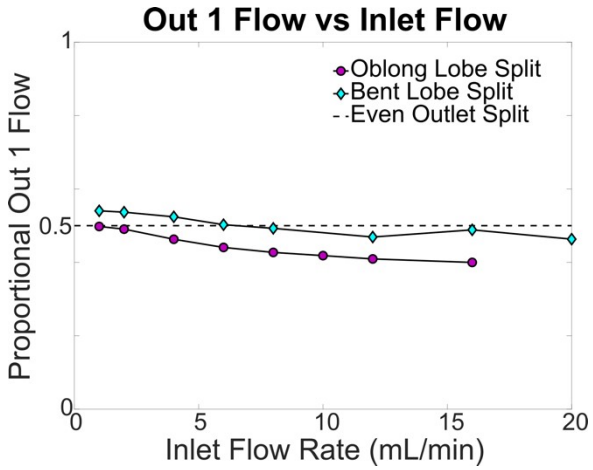

Supplemental Figure 3. Proportional Out 1 flow rate (Out 1 flow/Inlet flow) as a function of inlet flow rate. At each inlet flow rate, the Bent lobe device has proportional more fluid exiting through Out 1 than the Oblong lobe device.

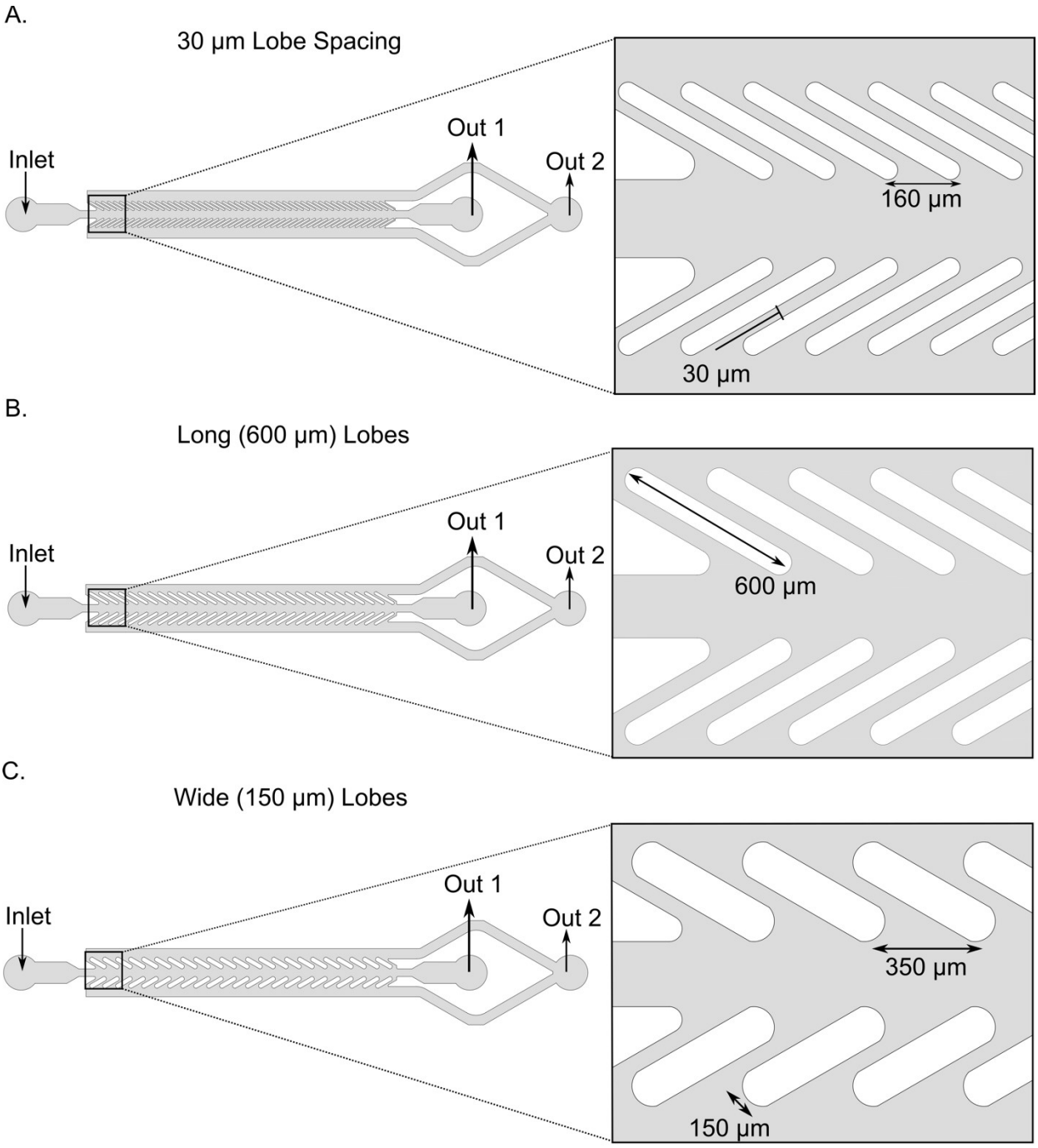

Supplemental Figure 4. Schematic of different variations of the oblong lobe filter design. The main dimension changes tested were **A.** 30 µm spacing between filter lobes, **B.** longer, 600 µm filter lobes, and **C.** wider, 150 µm filter lobes.

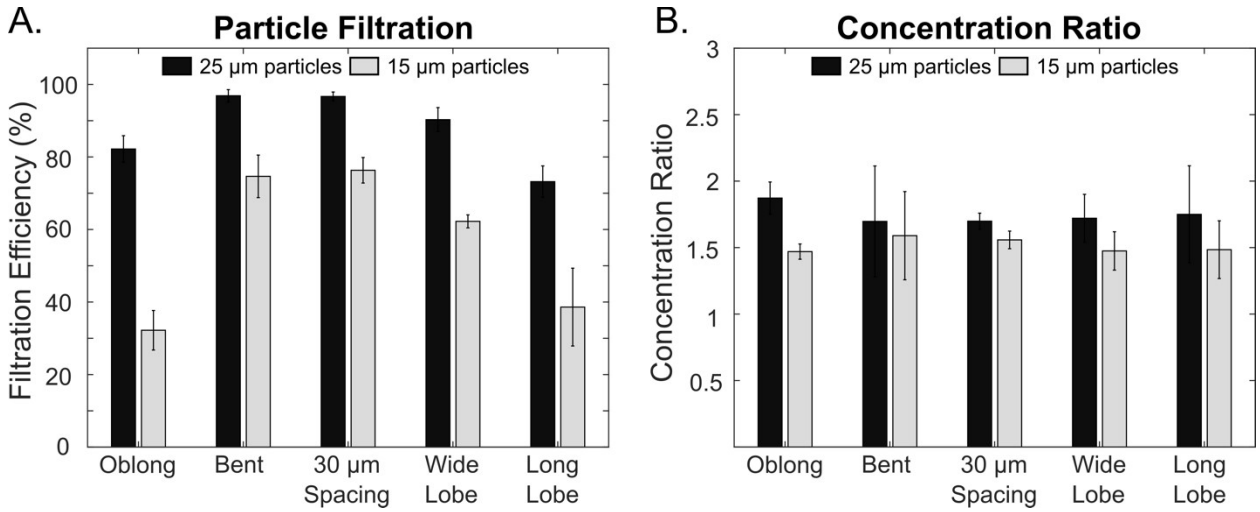

Supplemental Figure 5. Device performance metrics (**A.** Particle Filtration Efficiency and **B.** Concentration Ratio) from variations of the oblong lobe filter design (N = 3, error bars are standard deviation). The Bent lobe design and 30 µm spacing made the most drastic filtration performance increase. However, the 30 µm spacing device is much closer to 25 µm particles size, which will make the device prone to clogging or act as a crossflow filter.

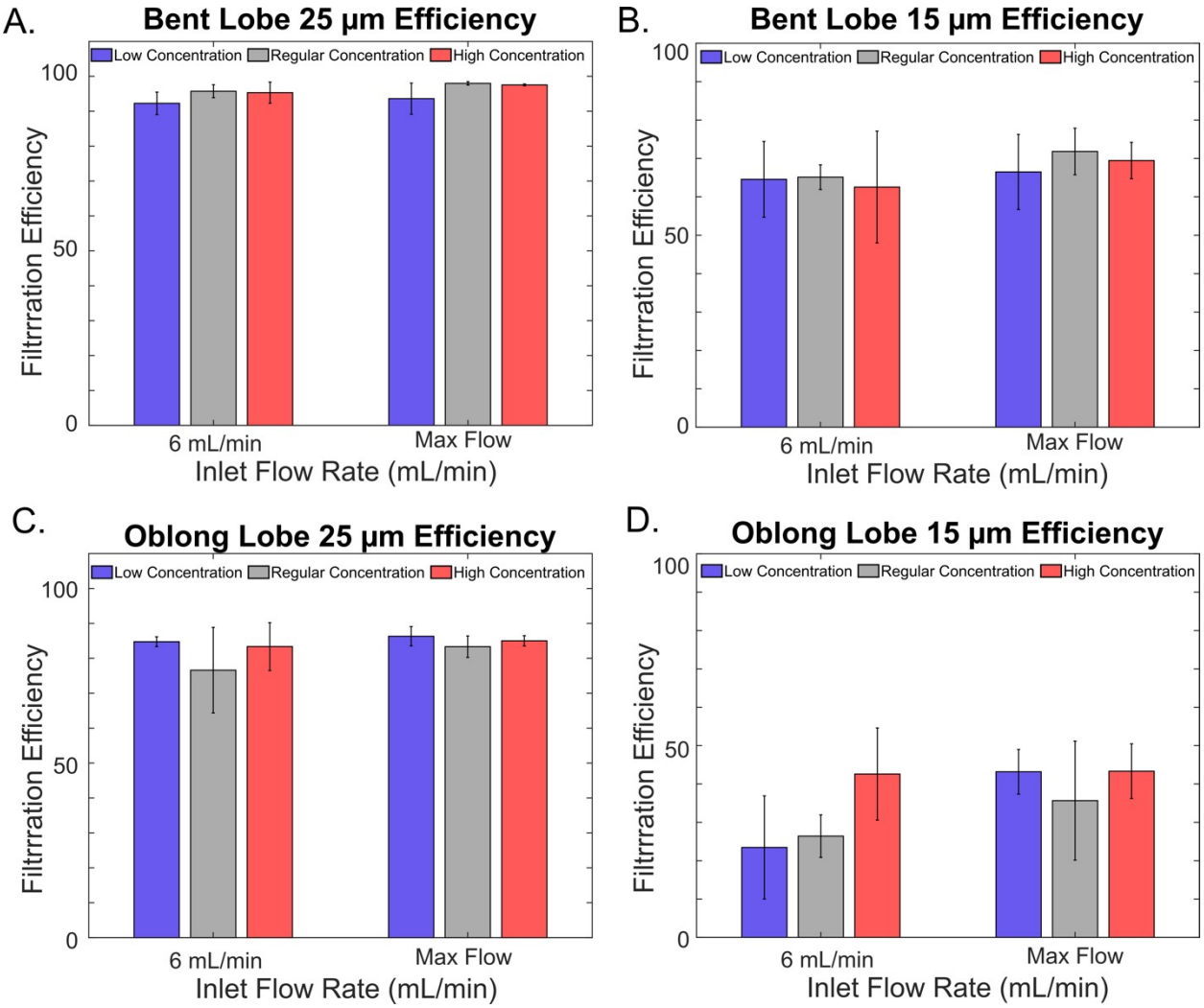

Supplemental Figure 6. Filtration efficiency for 25 µm and 15 µm particles across various particle suspension concentrations and flow rates for the **A/B.** Bent lobe and **C/D.** Oblong lobe designs. Both devices performed similarly across low (~10^4 particles/mL), regular (~10^6 particles/mL), and high (~10^7 particles/mL) at varying flow rates (N = 3, error bars are standard deviation). The max flow for the bent lobe device was 20 mL/min, while the max flow for the oblong lobe device was 16 mL/min.

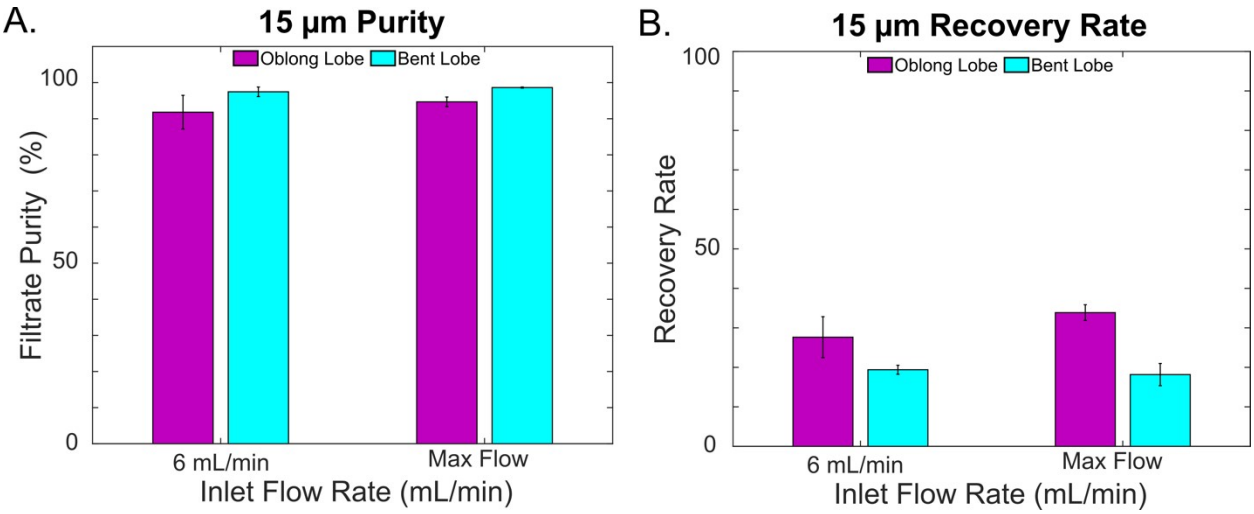

Supplemental Figure 7. A. Filtrate purity and **B.** Recovery rate for 15 µm particles at successful operational flow ranges for the oblong and bent lobe designs (N = 3, error bars are standard deviation). The max flow for the bent lobe device was 20 mL/min, while the max flow for the oblong lobe device was 16 mL/min.

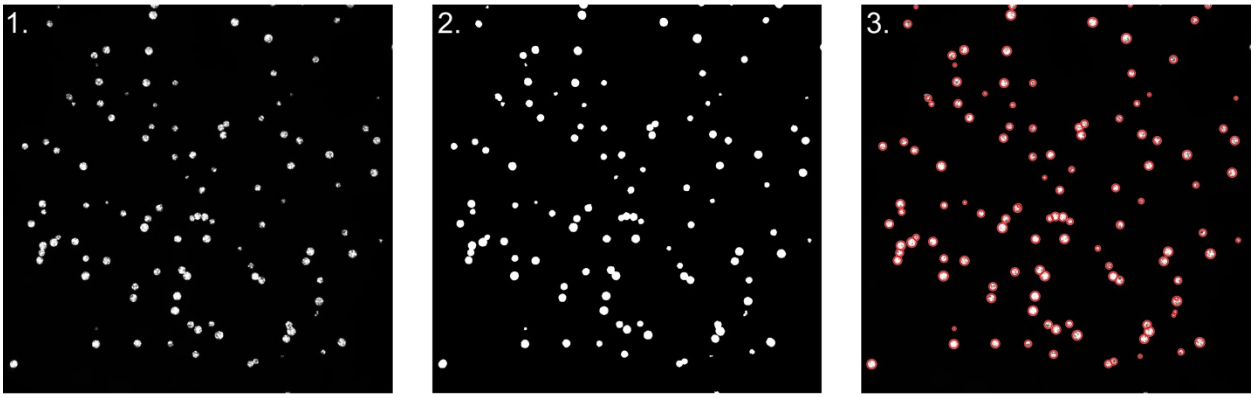

Supplemental Figure 8. Image processing algorithm used to obtain particle concentrations and particle sizes. 1. Original image obtained using GFP filter. 2. Images were binarized using imbinarize function in MATLAB. 3. Circles detected from image processing algorithm are shown in red. Radii were obtained and used for binning particle sizes for efficiency analysis.

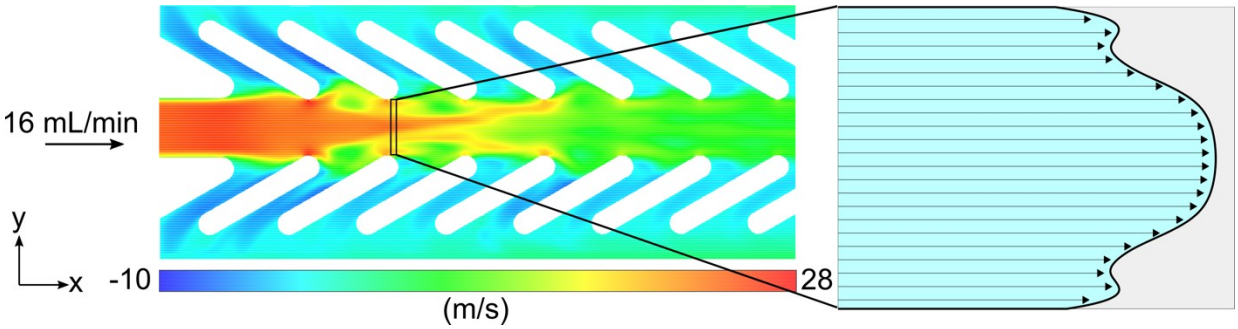

Supplemental Figure 9. Example velocity contours at high inlet flow rates for the Oblong lobe device. The complex velocity profile that has three local maxima and two inflection points was also observed.